Feature Article

Early View publication on
www.interscience.wiley.com
(issue and page numbers not yet assigned;
citable using Digital Object Identifier – **DOI**)

phys. stat. sol. (b), 1–14 (2005) / **DOI** 10.1002/pssb.200560960

Feature Article

Parametric amplification and polariton liquids in semiconductor microcavities

Jeremy J. Baumberg[*, 1] and **Pavlos G. Lagoudakis**[2]

[1] School of Physics and Astronomy, University of Southampton, Southampton, SO17 1BJ, UK
[2] Department of Physics and CeNS, University of Munich, Amalienstr. 54, 80799 Muenchen, Germany

Received 1 March 2005, revised 21 April 2005, accepted 27 April 2005
Published online 7 June 2005

PACS 42.50.–p, 42.65.-k, 71.36.+c, 78.45.+h, 78.67.–n

Parametric amplification in semiconductor microcavities provides an example in which nonlinear optical interactions produced by the exchange interaction of excitons become so large that multiple scattering of polaritons becomes important. Here we review time-resolved observations of the polariton interactions in a number of different geometries including pumping at either the magic angle, or the bottom of the polariton trap. Situations in which the polariton dispersion is multiply occupied by large populations give rise to $\boldsymbol{k}$-dependent energy shifts, modifying the dispersion dynamically, a situation we term the strongly-interacting 'polariton liquid'.

1 Introduction

The discovery of parametric amplification in semiconductor microcavities in 2000 has opened up a new highly-nonlinear optical regime to explore [1, 2]. Prior to this, optically-induced changes in the response of excitons in a semiconductor were at the level of a few per cent or less, before the photo-injected carriers screened the excitons into ionization. In semiconductor microcavities, the induced changes can be several thousand percent while still retaining the bound exciton [3]. This opens the way to exploring in some detail the nonlinear dynamics of excitons, and in particular of exciton–polaritons. Because polaritons with small kinetic energy live on a distorted dispersion relation, their dynamics is rather different to excitons, and can be directly observed [4].

Here, we explore some of the rich possibilities that emerge from the dynamics of polaritons. We aim to capture the broad feel of the phenomena through time resolved studies, which have been essential to clarify and disentangle the different scattering process that can occur. The predominant process is the pair scattering of two polaritons to different final states along the dispersion relation, which is constrained by the shape of the lower polariton dispersion [5]. We first review the simplest pair scattering, which occurs with the pump pulse incident at a 'magic' angle (in the language of non-linear optics, we would call this a triply phase-matched angle). We also explore the relationship between nonlinear optics and semiconductor quasiparticle scattering. We then show that multiple scattering plays a role and new 'nonlinear' polariton modes can appear, further distorting the dispersion [6]. Moving to a geometry in which the pump pulse is normally incident, we explore the way that the polariton dispersion can transiently distort, and propose a model in which the nonlinear interaction of light (of particular in-plane $\boldsymbol{k}$)

[*] Corresponding author: e-mail: j.j.baumberg@soton.ac.uk, Phone: +49 23 8059 3911, Fax: +49 23 8059 3910

with polaritons can be thought of in terms of a $\boldsymbol{k}$-dependent oscillator strength. We assume the reader is familiar with the strong-coupling regime of exciton–polaritons in a microcavity, and refer to previous reviews in this field [7].

2 Parametric scattering at the magic angle

2.1 Ultrafast experiments on semiconductor microcavities

Measuring the dynamics of polaritons in semiconductor microcavities requires an additional expansion of the tools of ultrafast spectroscopy. Undertaking angle-dependent measurements is vital to identify the different mechanisms involved in the scattering of these composite particles. Here we use two different techniques: angle-dependent pump–probe differential reflection/transmission, and angle-dependent luminescence analysed in a spectrometer or a streak camera. This required us to develop the first ultrafast goniometer in which several laser pulses can be adjusted in their incident angle on a sample without changing their time-delay. A number of implementations are possible in which the total path length travelled by each pulse remains constant while the incident angle (and hence $\boldsymbol{k}$) is tuned [8]. The microcavity samples here are cooled to 4 K using a wide field-of-view, cold-finger cryostat, allowing us to collect the light emission emerging at a range of angles.

Parametric scattering has been observed in a number of samples in our group, including InGaAs Multiple Quantum Wells (MQWs) in $3\lambda/2$ cavities, and GaAs Single Quantum Wells (SQWs) in λ and 2λ cavities. Many groups have also observed the effects in alternative strongly-coupled heterostructures, including II–VI microcavities [9, 10]. A number of questions remain open on the different efficiency of the scattering in different samples, including the effects of the number and placing of the quantum wells, the role of disorder both in the QW and the mirror stacks, as well as the composition. While the standard coupled mode theory [11] gives a good account of the angle- and detuning-dependence of the gain, it cannot account for the temperature-, heterostructure-, and disorder-dependence. To account for these effects it is then needed to consider scattering with all the exciton and polariton states in the microcavity. However, there still does not exist a good understanding of which states become occupied after excitation on the lower polariton branch. For instance, upper branch emission is also seen after lower branch excitation. Nor do we have a good understanding of how occupation of other states on the polariton dispersion affects pair scattering at the magic angle. An alternative treatment including all 2-exciton states has highlighted the role of nonlinear absorption at the idler in controlling the gain possible in the parametric amplification process [12].

2.2 Simple pair scattering

The simplest pair scattering process is one in which two polaritons at $\boldsymbol{k}_p$ mutually scatter to polaritons at $\boldsymbol{k} = 0, 2\boldsymbol{k}_p$ (Fig. 1 a). This process can only occur near the region of the lower polariton dispersion rela-

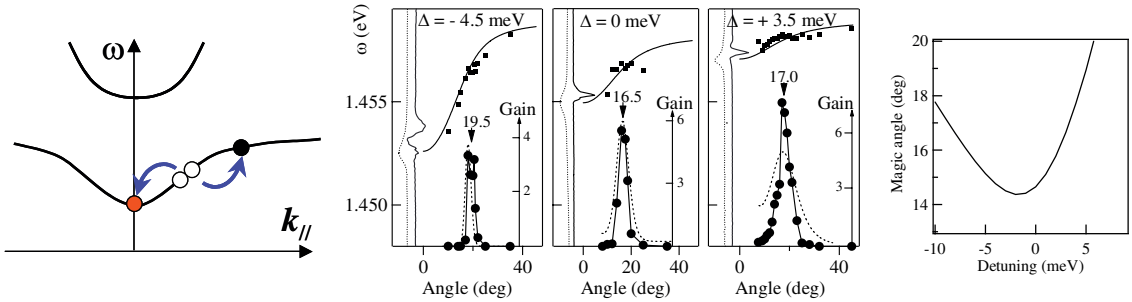

Fig. 1 (online colour at: www.pss-b.com) (a) Schematic magic angle parametric amplification, for final states at $\boldsymbol{k} = 0,2\,\boldsymbol{k}_p$. (b) Measured gain of a weak probe at normal incidence as a function of pump angle, for various detunings. (c) Optimum angle for gain as a function of detuning, for a typical InGaAs/GaAs microcavity.

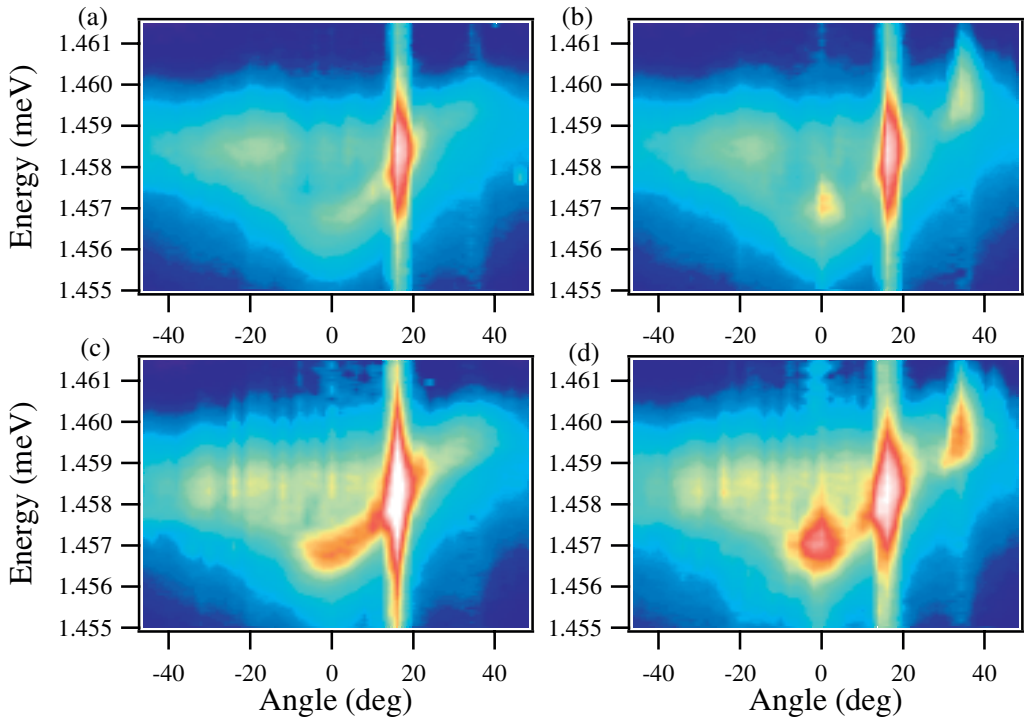

Fig. 2 (online colour at: www.pss-b.com) Time-integrated emission (log scale) from the lower polariton branch with incident pump pulse $\theta_{pump} = 16°$, when the normally-incident probe pulse is absent (a, c) or present (b, d), at low (a, b) 10 W/cm^2 or high (c, d) 30 W/cm^2 pump power.

tion, which satisfies energy and momentum conservation between initial and final states. This polariton region is given by the solution of $2E(\boldsymbol{k}_p) = E(0) + E(2\boldsymbol{k}_p)$. This can be clearly seen experimentally [1] when the gain of the normally incident probe pulse is measured as a function of the incident pump angle, at several detuning conditions between the cavity and the exciton resonance, $\Delta = E_c - E_x$ (Fig. 1b).

The optimum gain occurs at a magic angle which reaches a minimum near zero detuning (Fig. 1b, c), due to the way the shape of the dispersion changes with detuning. The strength of the pair scattering depends on the exciton fraction in the initial and final states and the strength of the dephasing of these states, and hence large positive or negative detuning conditions reduce the gain. Pair scattering is virtually absent on the upper polariton dispersion, or on the bare exciton dispersion, since the dispersion for these does not favour energy-momentum conservation.

To track the pair scattering process in more detail, the light emitted from the lower polariton branch is recorded over a wide range of angles, both in the spontaneous (no probe) and stimulated (with probe) regime (Fig. 2).

When the probe pulse is absent, polaritons scatter in pairs from the pump into a wide range of final states along the lower polariton dispersion [Fig. 2(a, c)]. The higher $\boldsymbol{k}$ states appear weaker because their photon fraction is smaller, so they escape more slowly from the microcavity, while the bigger exciton fraction of higher $\boldsymbol{k}$ states increases the probability of scattering to states outside the light cone. When the probe pulse is present, the pair scattering preferentially picks out the $\boldsymbol{k} = 0$ 'signal' state. This language of pump, signal (low energy) and idler (high energy) modes originates from optical parametric oscillator (OPO) theory. Occupation of a polariton state *increases* the probability of scattering into that state; there is a tendency for polaritons to accumulate in particular positions along the dispersion. The transition of the pair scattering from spontaneous in the absence of the probe to stimulated when the probe is present is a manifestation of the bosonic symmetry of the polariton wavefunction. The absence of such transi-

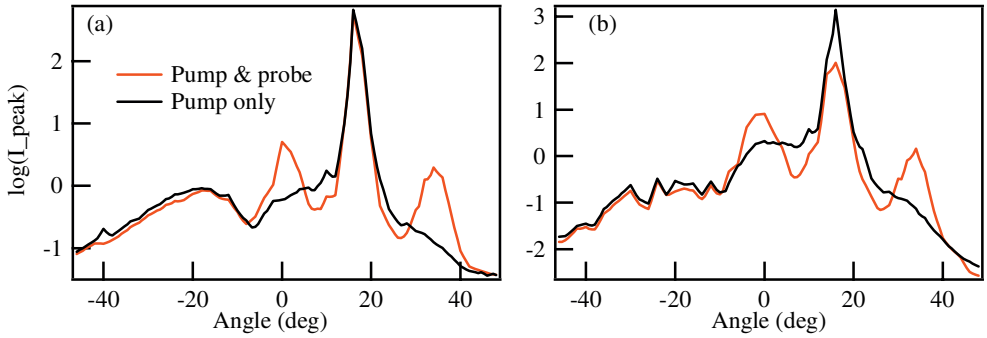

Fig. 3 (online colour at: www.pss-b.com) Maximum emission intensity at each angle (log scale) from Fig. 2, with and without the probe pulse at low (a) 10 W/cm^2 and high (b) 30 W/cm^2 pump power. Regions of resonant Rayleigh pump scattering, spontaneous parametric scattering and stimulated pair scattering are observed.

tions in bare quantum wells implies that polaritons are 'better' bosons (the lower energy polaritons have less multi-particle scattering mixed into their states) and paves the way for the study of polariton Bose condensation related phenomena [13–15]. The corresponding 'idler' polaritons are clearly visible at $2\boldsymbol{k}_p$ (Fig. 2, 3). However it is possible to note already a consistent feature of the idler polaritons, in that their energy spectrum and their wavevector distribution are considerably broader than that of the signal polaritons.

The other universal feature observed is the blue shift of the entire polariton dispersion when the strong pump injects significant polariton densities at the magic angle. This blue shift matches very well the simple theory, which is normally used to quantitatively describe the parametric scattering [16, 17]. Following this, it is possible to cast the equations for the coupling of the signal, idler and pump polaritons into a form which shows that new mixed states composed of both signal and idler experience the gain (Sec. 2.3). These mixed states are the eigenstates of the perturbed system and contain components from different in-plane wavevectors [18].

2.3 Quasimode theory of parametric amplification

In this section, we extend the theories developed for CW parametric scattering to the dynamic regime. We aim to find the transient eigenstates of the pair polaritons at each time, which independently experience the gain/loss. We assume a slowly varying polariton amplitude (which is a reasonable approximation for these narrow spectral linewidth cavities), and also work in the limit of negligible pump depletion (i.e. at low probe powers). In this case the equations governing the slowly-varying envelope of signal (S) and idler (I) can be written

$$\frac{\partial S}{\partial t} = -\gamma_S S - \Lambda I^* \ ,$$

$$\frac{\partial I^*}{\partial t} = -\gamma_I I^* - \Lambda^* S \qquad (1)$$

where $\Lambda(t) = iVP(t)^2\, \mathrm{e}^{i\nu t}$ accounts for the coupling. Here V is the exchange interaction between polaritons, P is the dynamic pump polariton occupation, and $\nu = 2\omega_P - \omega_S - \omega_I$ is the frequency mismatch from the magic angle condition. We look for solutions corresponding to gain: $S, I^* \propto \mathrm{e}^{qt}$. Solving the determinant of Eq. (1) produces the two solutions for the damping:

$$q_\pm = -\left(\frac{\gamma_S + \gamma_I}{2}\right) \pm \sqrt{\alpha^2 + |\Lambda|^2} \qquad (2)$$

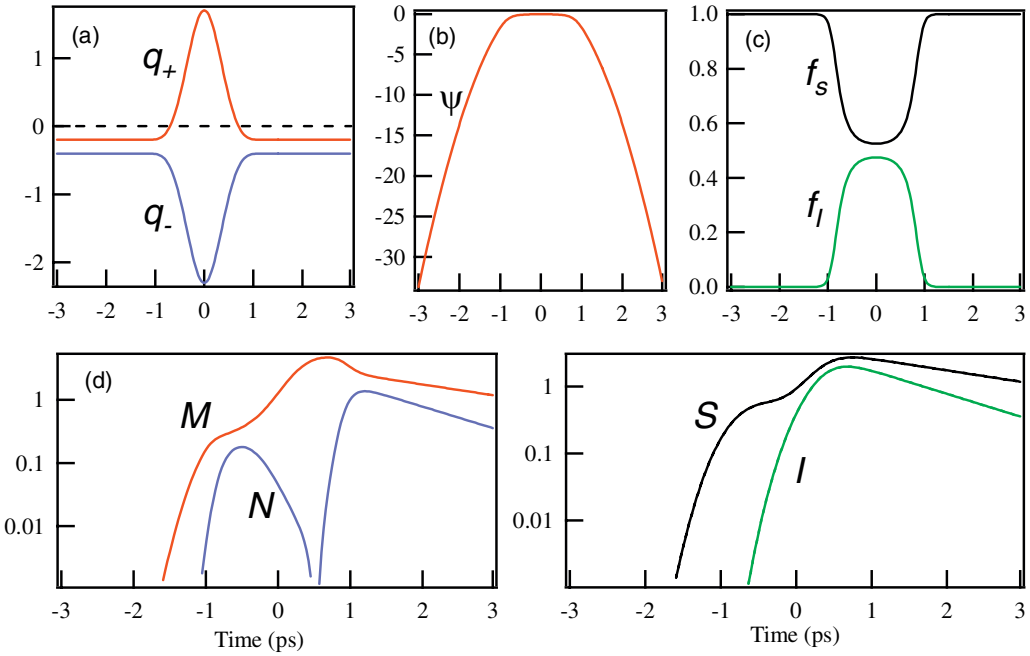

Fig. 4 (online colour at: www.pss-b.com) Quasimode calculations as a function of real time (ps) for (a) eigenvalues of *M, N*, (b) mixing parameter ψ, (c) fractional amount of signal and idler components in *M*, (d) dynamics of eigenmodes *M, N* and (e) of signal and idler, when the probe pulse is at $t = -1$ ps, pump at $t = 0$ ps.

with $\alpha = (\gamma_S - \gamma_I)/2$. These solutions are time dependent, with $q_\pm < 0$ away from the pump pulse corresponding to the individual damping of signal and idler. They repel strongly when the pump arrives, to produce transient gain ($q_+ > 0$, Fig. 4a). The eigenvectors of these solutions correspond to the two mixed modes (*M, N*) which experience these gains.

$$M = \frac{1}{\sqrt{1+\mathrm{e}^{2\psi}}}\left[-\mathrm{e}^{i\varphi}\, S + \mathrm{e}^{\psi}\, I^*\right]$$

$$N = \frac{1}{\sqrt{1+e^{2\psi}}}\left[\mathrm{e}^{\psi}\, S + \mathrm{e}^{i\varphi}\, I^*\right] \tag{3}$$

where we have defined $\sinh\psi = \alpha/|\Lambda|$ and $|\Lambda|\,\mathrm{e}^{i\varphi} = \Lambda$. This mixed complex transformation of the signal and idler is controlled by the phase mismatch, $\varphi = \nu t$, and a mixing parameter, $\psi(t)$.The mode *M* is amplified when the pump pulse arrives, while the mode *N* is de-amplified. The gain of these modes is given by $q_\pm = \bar{\gamma} \pm |\Lambda| \cosh\psi$, with the average damping, $\bar{\gamma} = (\gamma_S + \gamma_I)/2$. The incident probe couples into both modes, giving new instantaneously decoupled dynamical equations:

$$\frac{\partial M}{\partial t} = q_+ M - \frac{\mathrm{e}^{i\varphi}}{\sqrt{1+\mathrm{e}^{2\psi}}}\, S_{\mathrm{probe}}(t)\ ,$$

$$\frac{\partial N}{\partial t} = q_- N + \frac{\mathrm{e}^{\psi}}{\sqrt{1+\mathrm{e}^{2\psi}}}\, S_{\mathrm{probe}}(t)\ . \tag{4}$$

In the vicinity of the pump pulse, the modes *M, N* contain roughly equal admixtures of the signal and idler (Fig. 4c): in other words, when the pump is present, the true modes of the system are not *S, I* but

M, N. The dynamics of the quasi-uncoupled modes and the signal and idler are shown in Fig. 4d, e for a probe pulse which is 1 ps before the pump, and with damping of signal and idler, $\gamma_{s,i} = 0.2, 0.4$ meV corresponding to the experiments.

From these equations it can be seen that the amplification of the population of polaritons in the *M*-mode is roughly given by:

$$\left|\frac{M_{\text{out}}}{M_{\text{in}}}\right|^2 \approx \exp\left(2q_+T\right) \approx \exp\left(2|\Lambda|T\right) \approx \exp\left(2VI_{\text{pump}}T\right) \tag{5}$$

where T is the pulselength and I_{pump} is the pump power. This recovers the experimental result. It is also not what might be at first expected from a pair scattering process which in an uncoupled system would have a gain proportional to the *square* of the pump intensity. The completely mixed nature of signal and idler polaritons is what makes the parametric amplification so sensitive to dephasing of the idler component.

2.4 Multiple scattering at the magic angle

The above analysis shows that the parametric process creates new mixed pair states linked by the scattering with the strong pump. Effectively the strong pump acts to tie together polariton states in a pair-wise fashion. However, in pulsed experiments it is possible to transiently inject very large pump polariton densities, which in turn can lead to very large polariton densities at the signal and idler. These in turn act to tie together new pairs of polariton states, further distorting the polariton dispersion relation. We have previously analysed this case in some detail and summarise the results here to draw together the theme of parametric amplification.

If the data of Fig. 2(d) are analysed carefully it is possible to see additional polariton emission at positions which do not lie on the blue-shifted dispersion relation (Fig. 5) [6]. These directly correspond to the expected positions of new polariton branches created by 'dressing' the dispersion with signal, idler and pump polaritons. A number of off-branch modes have also now been observed under CW excitation [19].

Hence the meaning of the dispersion relation becomes more difficult to ascertain in the highly-nonlinear regime of parametric scattering in semiconductor microcavities. At any moment in time, a range of parametric interactions are available, whose strengths also control the ***k***-dependent self-energy shifts of the dispersion-relation. In turn, this modifies the allowed parametric interactions. This new regime of

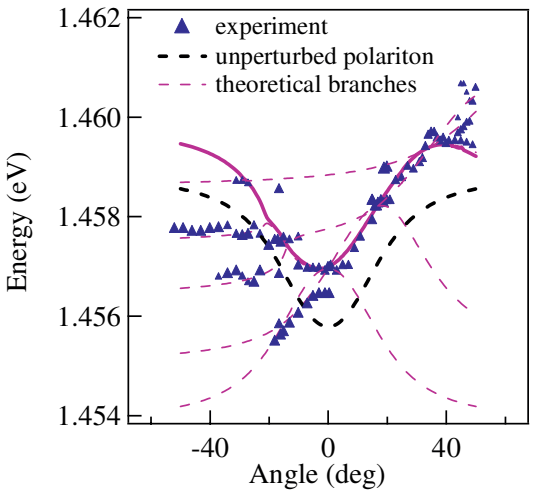

Fig. 5 (online colour at: www.pss-b.com) Extracted peak positions of emitted modes, with both pump and probe present (from Fig. 2d). Off-branch polaritons can be seen produced by renormalisation of the polariton dispersion under multiple scattering.

nonlinear optics more closely corresponds to the strong-coupling of He atoms in superfluidity, and could be termed a strongly-correlated '*polariton liquid*' [20, 21].

2.5 Double resonant on-branch multiple scattering

The experiments presented so far have concentrated on the simplest pair scattering situation with the probe pulse arriving at normal incidence. However, it is clear from the spontaneous scattering regime (eg. Fig. 2c) that many final pair states can satisfy energy-momentum conservation along the lower polariton dispersion. We describe now the results when the probe pulse is shifted to an angle of incidence of 6°, while the pump pulse remains at the magic angle of 17°. In this case we see not just the signal (S1) (as an amplified probe) and idler (I1) at 28° but a second signal beam (S2) emerging at an angle of –4° from the sample. Complementing these two signals is a second idler pulse (I2) at 42°. These results are summarized in Fig. 6.

Two possible routes exist for the pair scattering process to populate S2 and I2: either directly from the pump (P + P → S2 + I2), or from the coupled pair of signal and idler (S1 + I1 → S2 + I2). This process can be seeded either from the S2 (which can be populated by Rayleigh scattering of the initial signal) or from I2 (which is near degenerate with the exciton). This multiple scattering of coherent bosons can also

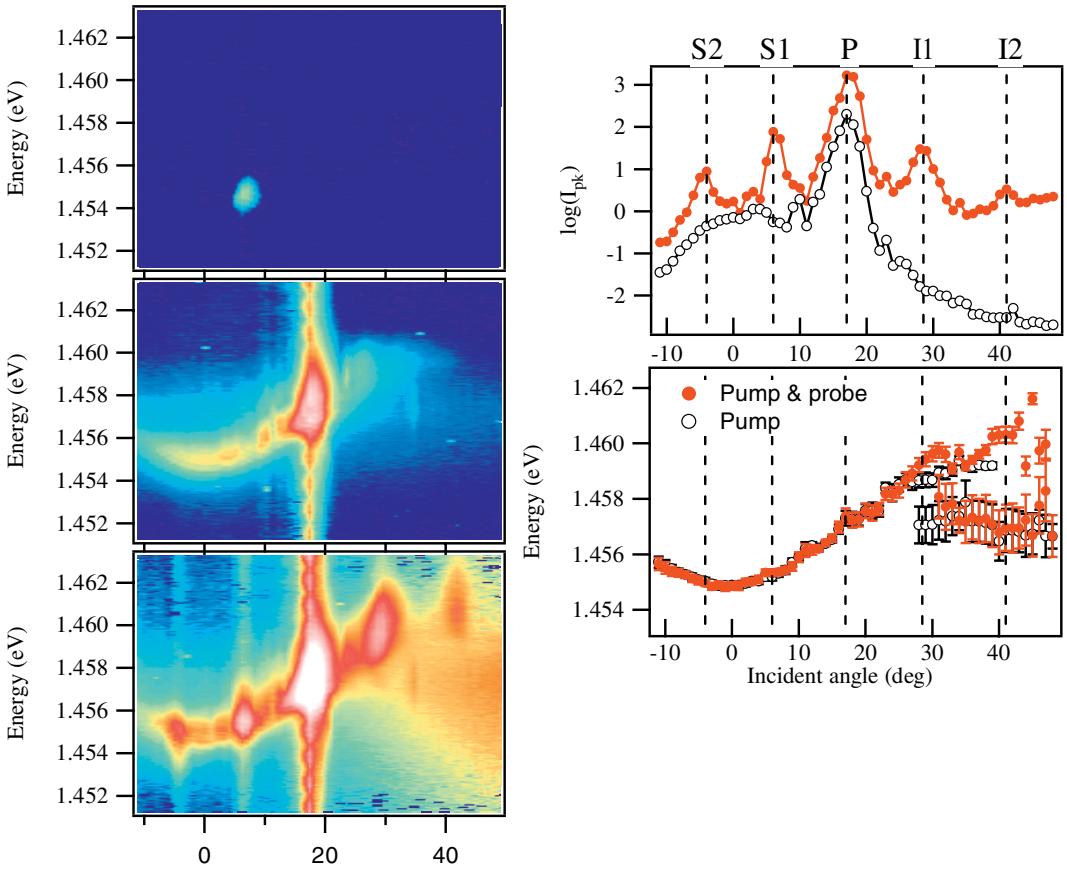

Fig. 6 (online colour at: www.pss-b.com) Lower polariton branch emission (on a log scale), for the three cases (a) probe alone at 6°, (b) pump alone at 17°, (c) both pump and probe incident. With the probe arriving away from $\boldsymbol{k} = 0$, new multiple scattering processes take place, giving rise to a second signal at –4° and a second idler at 42°. The gain for the signal is ~400 in these conditions.

be accounted for as the four-wave-mixing of pump and probe pulses, producing S2 and I1. In this equally valid description it is however less clear how to account for the strength of I2, which must arise from higher mixing. Both descriptions similarly treat the mixing of coherent bosonic fields, however four-wave-mixing retains coherence in the photon fields and polarizations, while the parametric scattering uses the polariton basis which more naturally accounts for the different properties of polaritons along the lower branch. The double-resonant pair scattering process seen here depends on all four states (S1, S2, I1, S2) being resonant on the polariton branches for its strength. This is only true for certain selected conditions of injected pump and probe polaritons, and for example does not work when the probe pulse arrives at –6°. In general, as the probe in-plane wavevector approaches that of the pump polaritons, the number of multiple scattering processes increases strongly, allowing many orders to be observed.

Another interesting question is the extent to which the modes S1, S2, I1, I2 form a new mixed polariton state with four components. It should be possible to probe intensity and phase correlations in the photons emitted from these states. In the Fourier domain, these correspond to spatial correlations in the polaritons inside the microcavity. However it is noticeable that the second idler is predominantly built of exciton states, and thus suffers very strong scattering processes. This may account for the large increase in emission from a broad range of lower energy states at high angles ($\theta > 40°$) when the multiple scattering process turns on. It is also possible that such broadband emission observed at large angles originates from localised exciton states (at smaller angles the strong emission from the pump and the polariton states in the trap hinders detection of light emitted from localised states that exist is small numbers). Under non-resonant excitation, emission from localised states can easily be observed and even lead to the appearance of a lasing mode due to the achievable population inversion in these low density states [22].

3 Local deformations of the dispersion: beyond pair scattering

The complete admixture of the idler in the mixed polariton state which is amplified explains the limitations of the parametric amplification. A number of careful experiments have compared how the gain changes with temperature, and number and type of quantum wells [23]. Two models have been advanced to account for this data, the first linking the increase in idler decoherence to the exciton binding energy, the second ascribing this to excitation induced dephasing of the pair-state to higher-lying continuum states [11, 12]. The common theme is clearly the proximity of the idler component of this mixed state to the very large density of excitons states (both localised and not) and unbound electronic states [24, 25]. One way to progress is thus to identify processes in which the idler can be energetically lower down inside the polariton trap, and thus better protected from these dephasing mechanisms.

A possible approach uses pump and probe beams at angles much closer to normal incidence, with all the scattering polaritons thus caught in the trap and so more stable against ionization and scattering. The problem is the small gain in this configuration due to the less advantageous shape of the dispersion for energy conservation in the pair scattering, and the short lifetime of polaritons before they escape as photons emitted from the sample [26, 27]. Only the broadening of the polariton mode in both energy and in-plane momentum caused by the finite lifetime of the cavity photons and diffraction in the planar microcavity allows the process to occur at all. This low gain is not predicted by the current models, which provide estimates for the polariton gain which are comparable or exceed those at the magic angle.

3.1 Polariton liquids at the bottom of the polariton trap

To explore the transient energy shifts during the pair scattering process, we collect the time-integrated transmission of pulses at different angles on the far side of the sample, and spectrally analyse it. We compare the results both with, and without, a probe pulse incident at $\theta_{\text{probe}} = 7°$ arriving simultaneously with the pump pulse which is at normal incidence. The polarization of the pump beam is linear while that of the probe beam is circular, in order to maximize the parametric amplification process [28, 29]. When the pump and probe arrive together, the scattering produces a gain of up to 15 of the probe beam, and a

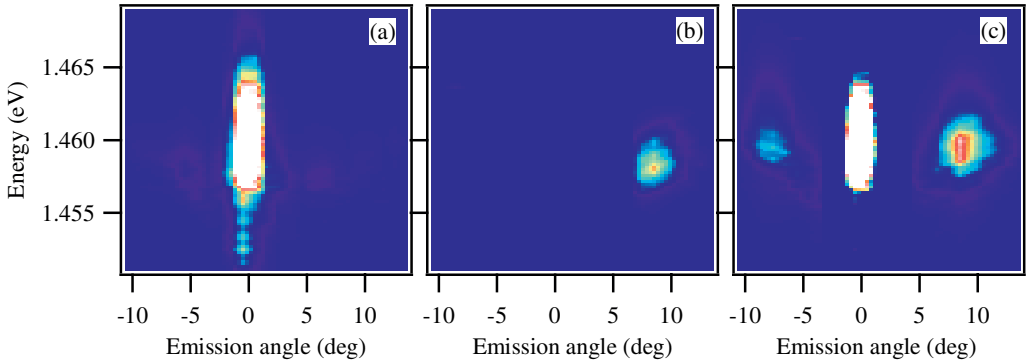

Fig. 7 (online colour at: www.pss-b.com) Time-integrated emitted light in transmission from the lower polariton, with the pump pulse normally incident, and the probe arriving at +7°. Parametric scattering is observed when both pulses arrive (c), producing an idler pulse at –7°. For comparison, pump alone (a) and probe alone (b).

similarly intense backscattered beam in the momentum-matched direction of $-\theta_{probe}$, which is the idler. The strength of the pair scattering driven by the pump depends on the cavity detuning from the exciton and is maximised for $\Delta = -1$ meV. To achieve this gain also depends on increasing the pump bandwidth (to several times the lower polariton linewidth) to allow resonance throughout the transient blue-shifting of the lower polariton branch. The angle dependent emission of pump, probe and phase-conjugate idler are clearly seen in Fig. 7 demonstrating the expected energy selectivity in the pair scattering process near the bottom of the polariton trap.

The parametric scattering process at the bottom of the trap nominally does not conserve energy-momentum, with a mismatch of 0.2 meV expected from the unperturbed dispersion. However this should be compared to the lower polariton linewidth for this sample at $\boldsymbol{k} = 0$, which is 0.5 meV. To gain an insight into the effects of the population-induced shifts in the dispersion, we extract the positions of peak emission and the emission strength as the pump power is varied by a factor of twenty (Fig. 8). Initially, it can be seen that increasing the pump power increases the signal and idler strength, however they rapidly saturate in intensity. On the other hand, the energy of the signal and idler continually blue shift with pump intensity. What is more surprising is that the the lower polariton branch at the bottom of the trap is rapidly deformed to a "w" shaped non-linear dispersion. Strong blue shifting appears where the pump, signal and idler are located. In the next section we discuss a model that tries to give some insight into these results.

It is also clear that these radical energy shifts can have a dramatic effect on the maximum possible gain observed (which is much less than expected). The gain can be clamped when the energy shifts pass beyond the condition for allowed energy-momentum scattering. At higher pump powers, it is clear that pair scattering at other points of the dispersion enables more states on the bottom of the polariton trap to become occupied. Once again this appears to be a situation more like that of the strongly-correlated polariton liquid.

3.2 Local oscillator strength model

One way to account for the data observed in the previous section is to treat the blue shifts as arising from the reduction in oscillator strength of the exciton component of the polariton. Since the Rabi splitting depends on the oscillator strength, the non-bosonic residual component of the polaritons which is sensitive to exciton densities can cause a reduction in the Rabi splitting, Ω. However we observe $\boldsymbol{k}$-dependent energy shifts which change with the polariton populations at each $\boldsymbol{k}$. We postulate that the admixture of exciton states in the polariton state at a particular $\boldsymbol{k}$, can correspondingly lead to the change of oscillator

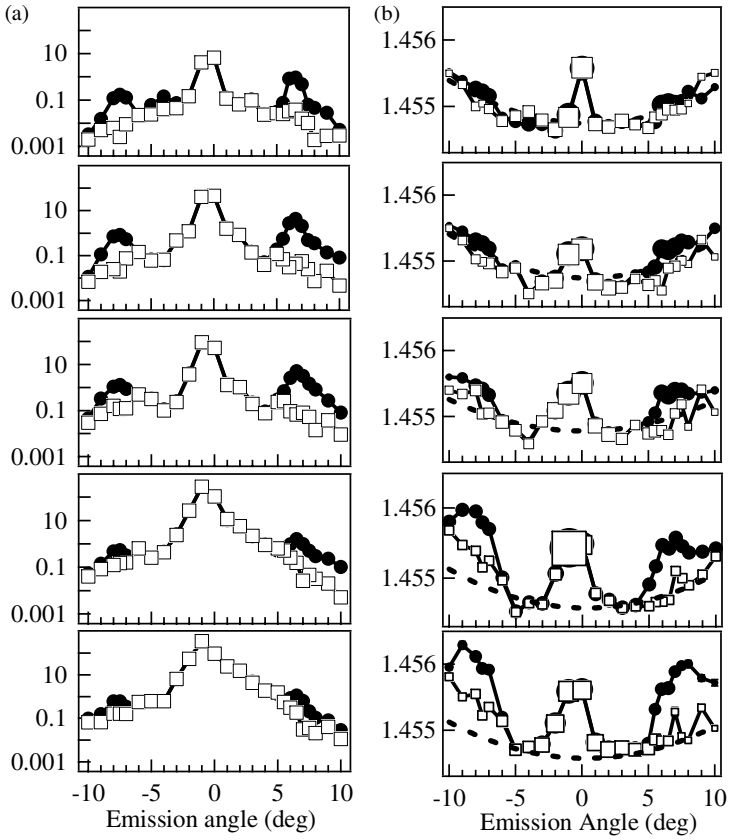

Fig. 8 Extracted peak emission strength (a) and peak emission energy (b) across the bottom of the lower polariton trap. The pump is at 0°, and probe at 7°, (open squares = pump only, solid circles = pump & probe), while the dashed line is the unperturbed lower polariton dispersion. The pump power increases from top to bottom, from 0.5 W cm^{-2} to 10 W cm^{-2}, while the probe power is kept constant.

strength for *only that admixture of excitons*. In other words, the oscillator strength which causes the Rabi splitting can be $\boldsymbol{k}$-dependent when it is the polaritons that are populated, $\Omega(k) \propto \sqrt{f[I(k)]}$.
The lower polariton energy is given by

$$\omega_p(k) = \tfrac{1}{2}\left[\omega_c(k) + \omega_x(k)\right] - \tfrac{1}{2}\sqrt{\left[\omega_c(k) - \omega_x(k)\right]^2 + \Omega(k)^2} \quad . \tag{6}$$

From this, the resulting fractional energy shifts are found to be comparable to the fractional change in oscillator strength $\Delta f/f$. This mechanism would imply that the upper polariton should also show an equivalent $\boldsymbol{k}$-dependent reduction in energy. However such experiments are hampered by the difficulty of observing the upper polariton simultaneously with the pump–probe parametric scattering – no emission is observed at the upper polariton, and injecting a probe here can radically modify the polariton scattering processes which occur.

Another possible way to account for the observations is that the emission we observe is time-integrated, and that the signal and idler polaritons emerge promptly when the pump polaritons are still in the sample (and thus the dispersion is blue-shifted), while the emission at other $\boldsymbol{k}$ occurs much more slowly at much later times after the pump polaritons have decayed from the sample (hence they emerge from the unshifted dispersion). The difficulty with this explanation is that all polaritons should show the same time dependence of emission – there are no non-resonant states excited which would contribute to

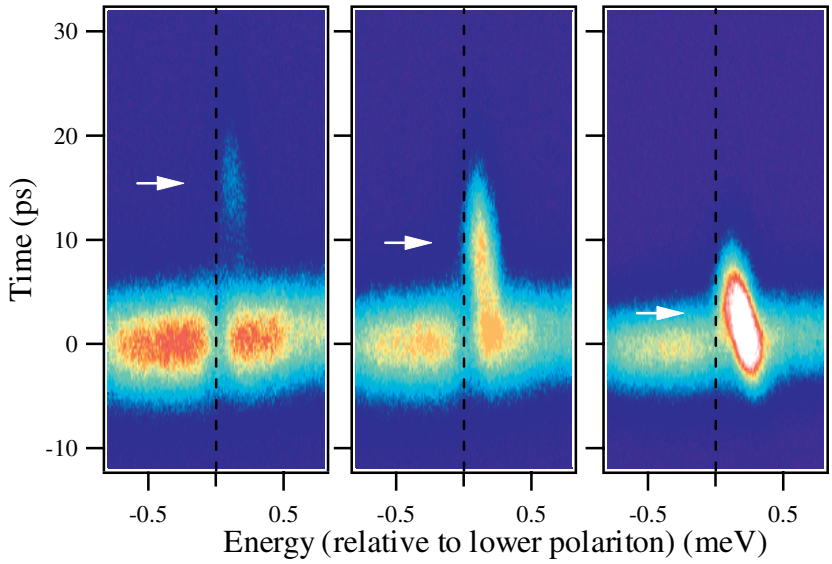

Fig. 9 (online colour at: www.pss-b.com) Streak camera directly-resolved $\boldsymbol{k} = 0$ emission when a normally-incident probe pulse arrives at time delays (t = 0 ps) close to the pump pulse (delayed at time marked by the arrow) which is at the magic angle. The dip in reflection is the lower polariton. The energy shifts of the $\boldsymbol{k} = 0$ polariton can be directly resolved. In (a) the pump pulse arrives after the probe pulse, and only weak gain is seen, at energies close to the polariton. In (c) the pump pulse is nearly simultaneous, and the gain is large, as is the energy shift.

delayed emission. However to verify this behaviour, it is necessary to directly time-resolve the emission during the parametric scattering as we show in the next section.

3.3 Direct time-resolved emission during parametric amplification

To directly resolve the dynamical energy-shifts during the parametric scattering process, we use a streak camera to track all the $\boldsymbol{k} = 0$ emission as a function of time together with a broadband 150 fs probe pulse which monitors the lower polariton occupation. We revert to the magic angle geometry (Section 2.2) in these preliminary experiments, and vary the time delay between the pump and probe pulses on the microcavity (Fig. 9). The signal light emerging from the microcavity at normal incidence after the probe pulse is reflected is directly resolved in time – the dip in the reflected spectrum at $t = 0$ ps is the lower polariton branch. When the pump pulse arrives close in time, a portion of the probe pulse becomes amplified. Clearly visible is the chirp in the signal (or parametrically-amplified probe): the blue-shift is initially large and reduces as time progresses as the pump polaritons are depleted and escape from the sample. The chirp is reduced as the pump pulse arrives at later times. Further experiments are underway to explore the parametric scattering described above, in the polariton liquid regime, to try and disentangle the different processes occurring.

4 Historical perspective (JJB)

For this special issue reviewing our research on semiconductor microcavities, it is perhaps worthwhile to reflect on how we stumbled upon the enormously-strong parametric scattering process in semiconductor microcavities. Since the pioneering work of Arakawa and Weisbuch in identifying the strong coupling regime in these structures, much excellent work in the 1990s at EPFL, Sheffield and elsewhere had gone into understanding how luminescence emerges from the two polariton branches. From my background in ultrafast spectroscopy of semiconductors, it was natural to try and understand the dynamics of polaritons.

However one of the most frequent assumptions always made previously in the study of *any* semiconductor heterostructure was that the angle of incident and emitted light is decoupled from any dynamics in the sample, essentially because the lowest energy exciton states observed are relatively localised in space.

Initial experiments that I undertook at Hitachi Cambridge in 1997 in collaboration with the Sheffield group thus used a conventional geometry in which incident pump and probe beams were a few degrees from normal incidence thus observing polaritons only around $\boldsymbol{k} = 0$. The results from these experiments were truly puzzling. Among the crucial observations was that the precise pump spectrum used made a huge difference to both the time-resolved reflectivity, and the four-wave mixing dynamical signatures. By using coherent pulse shaping with real-time spectral filtering [30], we were able to deduce that not only were there drastic differences between pumping the upper polariton alone, and pumping the lower polariton alone, but also when pumping both branches together. Even more surprising, was when pumping the lower polariton simultaneously with states at $\boldsymbol{k} = 0$ at higher energy up to the exciton energy (even though there is no direct absorption into polaritons) produced a markedly different signal. This work signalled that something remarkably odd was sensitive in the polariton system, and on moving the group to Southampton in 1998, I set out to try and understand what this could be.

Research at Sheffield beautifully depicted the angle-dependence of the polariton branches, and I began to wonder about $\boldsymbol{k}$-selection rules in the system. In particular, the identification of a bottleneck in relaxation of lower polaritons which reduces the rate at which higher-$\boldsymbol{k}$ excitons relax into the lower branch $\boldsymbol{k} = 0$ polaritons suggested that the dynamics would be interesting. Hence I decided to attempt angularly-sensitive pump–probe experiments. To do this required development of a new piece of apparatus for femtosecond spectroscopy since normal beamline geometries had the unfortunate effect of changing the time delay every time the angle of incidence was changed. The femtosecond goniometer that we developed had a nice property that the temporal overlap of pump and probe pulses was preserved (within about 100 fs) as the pump and probe angles were freely adjusted, allowing simple comparison of dynamics at different angles, and hence different polariton in-plane $\boldsymbol{k}$. Pavlos Savvidis, my first PhD student at Southampton took on the job of measuring the response when pumping higher-$\boldsymbol{k}$ polaritons to see how quickly they could relax to $\boldsymbol{k} = 0$, where they were probed by a second weak pulse. It was during these first initial runs that Pavlos came to me saying there was something peculiar ('wrong') with the data. At certain pump incident angles, the dynamical response changed sign from giving a small pump-induced decrease in the probe reflectivity to giving a vast increase. More puzzling, under investigation, it transpired that more probe light could be reflected from the sample when the pump arrived, than was actually incident on the sample. (This is rather easy to measure since the microcavity reflectivity off the polariton branches is close to 100%). At this point it was clear that some new process which was particularly angular-resonant was occurring, and we rapidly mapped out the angular-, spectral- and ultrafast-spectroscopy to reveal the classic magic-angle parametric scattering process.

One remaining note in this story is salutary. The original paper that we submitted to Physical Review Letters [1] also discussed the spin-selection rules for the parametric scattering. Experimentally we had observed that seeding the stimulated scattering required the *opposite* probe circular polarisation to the pump. The incredulity of the referee to this physics forced us to check repeatedly this fact. However the point about the stimulated scattering is that it is so very strong that an extremely weak probe pulse is necessary, on the order of microwatts. Hence the process of checking directly the circular polarisation helicity of the probe was always done by increasing the probe power and rotating a half-wave plate before a polarisation beam splitter which split the pump–probe beamlines. Typically such optics are imperfect at the level of 10^{-4} and, having confirmed the helicity of the probe, we reduced the probe power assuming that the helicity remained unchanged. The severe scepticism of Benoit Deveaud to our findings eventually forced us to track down the background amount of opposite helicity only present at low probe powers, and confirm the expected intuition of spin-conserving parametric scattering. Interestingly, subsequent research by Pavlos Lagoudakis in the group uncovered a far more complicated story of spin in the parametric scattering process which was partly triggered by the ideas discussed when trying to reconcile such peculiar spin observations.

There are several observations to be taken from the semiconductor microcavity field. Firstly, just because a research sub-topic slows down does not mean that there is not huge life still to be teased out of it. Too quick an opportunistic redirecting of research towards the latest sexy topic will miss much of the physics. Secondly, I realise how little I understood about excitonic states in quantum wells until forced to confront the issues when they are embedded in microcavities. The direct access to states of different $\boldsymbol{k}$ which are here separated clearly in energy provides a spectacular window on the excitonic state. I still understand less about the quantum well electronic states than about the coupled exciton–photons in the microcavity, but I think much progress has been made, visible throughout the papers collected here. Thirdly, the physics opened up by exploring parametric scattering is an excellent paradigm of research in action, and an excellent demonstrator of the breadth of quantum optoelectronics: the connection between Bose-condensation of quasiparticles in the solid state, and the technological application of ultrafast ultra-high-gain micro-parametric oscillators and amplifiers is not an obvious one. Currently these are still vibrant and open questions.

Acknowledgements We would like to thank Delores Martin-Fernandez, Cristiano Ciuti, and Pavlos Savvidis for the results and ideas they contributed, and Maurice Skolnick and David Whittaker for long-term collaboration, samples and many fruitful discussions.

References

[1] P. G. Savvidis, J. J. Baumberg, R. M. Stevenson, M. S. Skolnick, D. M. Whittaker, and J. S. Roberts, Phys. Rev. Lett. **84**, 1547 (2000).
[2] R. M. Stevenson, V. N. Astratov, M. S. Skolnick, D. M. Whittaker, M. Emam-Ismail, A. I. Tartakovskii, P. G. Savvidis, J. J. Baumberg, and J. S. Roberts, Phys. Rev. Lett. **85**, 3680 (2000).
[3] M. Saba, C. Cuiti, J. Bloch, V. Thierry-Mieg, R. Andre, Le Si Dang, S. Kundermann, A. Mura, G. Bongiovanni, J. L. Staehli, and B. Deveaud, Nature **414**, 731 (2001).
[4] R. Houdré, C. Weisbuch, R. P. Stanley, U. Oesterle, P. Pellandini, and M. Ilegems, Phys. Rev. Lett. **73**, 2043 (1994).
[5] P. G. Savvidis, J. J. Baumberg, R. M. Stevenson, M. S. Skolnick, J. S. Roberts, and D. M. Whittaker, Phys. Rev. B **62**, R13278 (2000).
[6] P. G. Savvidis, C. Ciuti, J. J. Baumberg, D. M. Whittaker, M. S. Skolnick, and J. S. Roberts, Phys. Rev. B **64**, 075311 (2001).
[7] "Special Issue on Microcavities", edited by J. J. Baumberg and L. Vina, Semicond. Sci. Technol. **18**, S279 (2003).
G. Khitrova et al., Rev. Mod. Phys. **71**, 1591 (1999).
M. S. Skolnick, T. A. Fisher, and D. M. Whittaker, Semicond. Sci. Technol. **13**, 645 (1998).
A. Kavokin and G. Malpuech, Cavity Polaritons (Elsevier, Amsterdam, 2003)
[8] P. G. Savvidis and P. G. Lagoudakis, Semicond. Sci. Technol. **18**, S311 (2003).
[9] A. Huynh, J. Tignon, O. Larsson, P. Roussignol, C. Delalande, R. Andre, R. Romestain, and L. S. Dang, Phys. Rev. Lett. **90**, 106401 (2003).
[10] M. Muller, R. Andre, J. Bleuse, R. Romestain, L. S. Dang, A. Huynh, J. Tignon, P. Roussignol, and C. Delalande, Semicond. Sci. Technol. **18**, S319 (2003).
[11] C. Ciuti, P. Schwendimann, and A. Quattropani, Semicond. Sci. Technol. **18**, S279 (2003).
[12] S. Savasta, O. Di Stefano, and R. Girlanda, Semicond. Sci. Technol. **18**, S294 (2003).
[13] D. Porras, C. Ciuti, J. J. Baumberg, and C. Tejedor, Phys. Rev. B **66**, 085304 (2002).
[14] H. Deng, G. Weihs, C. Santori, J. Bloch, and Y. Yamamoto, Science **298**, 199 (2002).
[15] G. Weihs, H. Deng, R. Huang, M. Sugita, F. Tassone and Y. Yamamoto, Semicond. Sci. Technol. **18**, S386 (2003).
[16] C. Ciuti, P. Schwendimann, B. Deveaud, and A. Quattropani, Phys. Rev. B **62**, R4825 (2000).
[17] C. Ciuti, P. Schwendimann, and A. Quattropani, Phys. Rev. B **63**, 041303 (2001).
[18] C. Ciuti, Phys. Rev. B **69** 245304 (2004).
[19] A. I. Tartakovskii, D. N. Krizhanovskii, D. A. Kurysh, V. D. Kulakovskii, M. S. Skolnick, and J. S. Roberts, Phys. Rev. B **65**, 081308 (2002).

[20] L. Tisza, Phys. Rev. **72**, 838 (1947).
[21] O. Penrose and L. Onsager, Phys. Rev. **104**, 576 (1956).
[22] P. G. Lagoudakis, M. D. Martin, J. J. Baumberg, G. Malpuech, and A. Kavokin, J. Appl. Phys. **95**, 8979 (2004).
[23] M. Saba, C. Ciuti, S. Kundermann, J. L. Staehli, and B. Deveaud, Semicond. Sci. Technol. **18**, S325 (2003).
[24] P. G. Lagoudakis, M. D. Martin, J. J. Baumberg, A. Qarry, E. Cohen, and L. N. Pfeiffer, Phys. Rev. Lett. **90**, 206401 (2003).
[25] A. Qarry, G. Ramon, R. Rapaport, E. Cohen, A. Ron, A. Mann, E. Linder, and L. N. Pfeiffer, Phys. Rev. B **67**, 115320 (2003).
[26] F. Quochi, C. Ciuti, G. Bongiovanni, A. Mura, M. Saba, U. Oesterle, M. A. Dupertuis, J. L. Staehli, and B. Deveaud, Phys. Rev. B **59**, R15594 (1999).
[27] G. Messin, J. P. Karr, A. Baas, G. Khitrova, R. Houdre, R. P. Stanley, U. Oesterle, and E. Giacobino, Phys. Rev. Lett. **87**, 127403 (2001).
[28] P. G. Lagoudakis, P. G. Savvidis, J. J. Baumberg, D. M Whittaker, P. R. Eastham, M. S. Skolnick, and J. S. Roberts, Phys. Rev. B **65**, R161310 (2002).
[29] A. Kavokin, P. G. Lagoudakis, G. Malpuech, and J. J. Baumberg, Phys. Rev. B **67**, 195321 (2003).
[30] J. J. Baumberg, A. Armitage, M. S. Skolnick, and J. Roberts, Phys. Rev. Lett. **81**, 661 (1998).